



INVITED ARTICLE

Subduction and carbonate platform interactions

Sabin Zahirovic¹ | Ahmed Eleish² | Sebastiano Doss¹ | Jodie Pall¹ |
John Cannon¹ | Mattia Pistone³ | Michael G. Tetley^{4,5} | Alex Young⁶ | Peter Fox²

¹EarthByte Research Group, School of Geosciences, The University of Sydney, Sydney, NSW, Australia

²Tetherless World Constellation, Rensselaer Polytechnic Institute, Troy, NY, USA

³Department of Geology, University of Georgia, Athens, GA, USA

⁴Laboratoire de Géologie de Lyon, Université Claude Bernard Lyon 1, Lyon, France

⁵University of Texas Institute for Geophysics, Jackson School of Geosciences, The University of Texas at Austin, Austin, TX, USA

⁶GeoQuEST Research Centre, School of Earth, Atmospheric and Life Sciences, University of Wollongong, Wollongong, NSW, Australia

Correspondence

Sabin Zahirovic, EarthByte Research Group, School of Geosciences, The University of Sydney, NSW 2006, Australia.
Email: sabin.zahirovic@sydney.edu.au

Funding information

Alfred Sloan Foundation, Grant/Award Number: G-2017-9997 and G-2018-11296; Australian Research Council, Grant/Award Number: DE210100084; Ambizione Fellowship of the Swiss National Science Foundation and UGA Presidential Funds, Grant/Award Number: PZ00P2_168166; Australian National Collaborative Research Infrastructure System; H2020 European Research Council, Grant/Award Number: 617588

Abstract

Plate tectonics, as the unifying theory in Earth sciences, controls the functioning of important planetary processes on geological timescales. Here, we present an open-source workflow that interrogates community digital plate tectonic reconstructions, primarily in the context of the planetary deep carbon cycle. We present an updated plate tectonic reconstruction covering the last 400 million years of Earth evolution and explore components of the plate–mantle system that is involved in the exchange and storage of carbon. First, the workflow enables us to estimate subduction zone lengths through time, which represent the “tap” of carbon that is released at convergent tectonic margins. Second, we explore the role of Andean-style versus intra-oceanic subduction regimes during Pangea assembly and breakup. Third, we provide an improved model for carbonate platform evolution since the Devonian and evaluate the interaction of subduction zones and buried carbonate platforms. Last, we present a new model for estimating oceanic age, carbon content in the upper oceanic crust, and estimated (carbon-containing) sediment thicknesses through time and present methods to track the subduction of this material through time. These components of the deep carbon cycle are key mechanisms controlling, or at least modulating, atmospheric CO₂ on geological timescales and hence strongly influencing long-term climate. We find that the mid to Late Cretaceous greenhouse climates were likely driven by increased subduction fluxes of volatiles and increased subduction zone interactions with carbonate platforms in the Tethyan tectonic domain. Our work highlights the importance of community digital plate tectonic reconstructions as a framework for studying key systems, such as the deep carbon cycle, that influence the life-support mechanisms on our planet.

KEYWORDS

carbon cycle, carbonate platforms, plate motions, subduction, tectonics

This is an open access article under the terms of the Creative Commons Attribution License, which permits use, distribution and reproduction in any medium, provided the original work is properly cited.

© 2022 The Authors. *Geoscience Data Journal* published by Royal Meteorological Society and John Wiley & Sons Ltd.

1 | INTRODUCTION

Plate tectonics, as the unifying theory in Earth sciences, helps contextualize geological data to provide insights on fundamental planetary processes that are driven by the convecting mantle and the moving tectonic plates on the surface. A key to the planetary life-support systems on Earth is the “deep carbon cycle” where carbon is stored and exchanged between the mantle, lithosphere, and surface reservoirs (Dasgupta & Hirschmann, 2010; Plank & Manning, 2019). Mantle flow and plate tectonic processes have modulated atmospheric CO₂ and other greenhouse gas levels on geological timescales, while other geological processes, such as silicate weathering, have resulted in drawdown and return of CO₂ into the solid Earth (Lee et al., 2019). These processes have been important drivers of deep-time climate transitions between icehouse and greenhouse states (Dutkiewicz et al., 2018; Isson et al., 2020) and have fundamental influences on, and relationships with, life on our planet (Sleep & Zahnle, 2001).

Although imperfect, particularly in deeper time (such as in pre-Pangea times), the geological record provides key constraints on Earth's past. By synthesizing geological and geophysical data, plate tectonic reconstructions can be constructed, which can often be used to fill spatiotemporal gaps in the geological record and in our understanding of key planetary processes. The open-source and cross-platform GPlates (www.gplates.org) software (Müller et al., 2018) has been used to create a range of community plate tectonic reconstructions (Domeier & Torsvik, 2014; Matthews et al., 2016; Müller et al., 2019; Zahirovic et al., 2016). These digital plate motion models can be interrogated with tectonic parameters (e.g., slab flux, interactions with crustal carbonates, etc.) that can be used to infer the deep carbon cycle evolution of our planet (Dutkiewicz et al., 2018; East et al., 2020; Johansson et al., 2018; Merdith et al., 2019; Pall et al., 2018; Wong et al., 2019). To overcome the simplifying assumption of plate rigidity, a number of models now include deformation of the lithosphere (Cao et al., 2020; Gurnis et al., 2018; Liu et al., 2017; Müller et al., 2019), further enhancing the usability of these models in tracking the evolution of rifted basins, orogenic systems, and implications for paleobiogeography and climate. The accuracy of plate tectonic reconstructions can deteriorate deeper into the geological past, largely due to the lack of preserved or sampled geological constraints. The last ~250 Ma are best constrained due to preserved seafloor spreading records (at least in the Indo-Atlantic realm). However, continental paleomagnetism can be used to infer synthetic seafloor spreading for earlier times, but only where the terrane motions are primarily latitudinal. Where these constraints are lacking, other geological proxies of prior geographic affinity, coupled to

evidence from sedimentary, metamorphic, and igneous data, are used to create probable, and often non-unique, reconstructions.

The models, associated data, and workflows to interrogate the models represent an important resource for a number of disciplines within and beyond Earth sciences (e.g., paleobiogeography, biological evolution, paleoclimate, etc.). Here, we present a toolkit to measure subduction zone lengths, track the interaction of carbonate platforms in the overriding crust with subduction zones, automatically characterize Andean-style versus intra-oceanic subduction, and estimate the bulk CO₂ content of the subducting upper oceanic crust from the GPlates plate reconstructions, highlighting the power and flexibility of a digital representation of the Earth's evolving tectonic system.

2 | METHODS, DATASETS, AND MODELS

2.1 | GPlates plate tectonic reconstruction models

GPlates is a cross-platform and open-source desktop software for the interactive construction, modification, and visualization of plate tectonics, paleogeography, and mantle structure (Müller et al., 2018). GPlates is a deep-time geographic information system (GIS), that can handle vector, raster, and three-dimensional (3D) volume visualizations. The pyGPlates Python application programming interface (API) can be used to automate many of the vector-based functionalities of GPlates, such as interrogating plate reconstructions (also known as plate motion models) and spatiotemporal analyses of the plate kinematics. For the time of the Pangea supercontinent dispersal (~250 Ma to present), seafloor spreading histories from the preserved oceanic crust provide a relatively high level of confidence for relative plate motions where they are available. For times before Pangea, continental paleomagnetic data supplemented by geological evidence and kinematic ‘rules’ (Williams et al., 2015; Zahirovic et al., 2015) are used to constrain the motions of most major continental blocks.

In this study, the Matthews et al. (2016) plate motion model is presented for the last 410 million years, which combines the Müller et al. (2016) model detailing plate motion between 0 and 230 Ma and the Domeier and Torsvik (2014) plate motion model for times between 410 and 250 Ma. In this study, we also consider a correction to the absolute plate motion of the Pacific Plate, as described by Torsvik et al. (2019). For the subducting plate area, subducting sediment volumes, and subducting oceanic crustal

carbon, we also present an analysis of more recent plate reconstructions. We analyze a new hybrid plate motion model (Model Z2021-MCY); a merge of the Young et al. (2018) (410–250 Ma), the Müller et al. (2019), and Cao et al. (2020) (250–0 Ma) plate reconstructions, with some minor modifications. Pre- and post-Pangea plate reconstructions have typically relied on different combinations of geological constraints. Notably, post-Pangea models make greater use of hotspot reference frames, especially in the last 100 million years (Ma), while deeper-time models rely more on paleomagnetic reference frames. To “stitch” such models together temporally, one has to first apply either the same paleomagnetic reference frame or merge with another paleomagnetic reference frame with similar underpinnings (i.e., ensure consistency in approach, especially with respect to the inclusion or exclusion of True Polar Wander). Following this merge of pre- and post-Pangea global kinematics in a paleomagnetic frame, an optimization of the absolute reference frame can attempt to minimise True Polar Wander, with the aim of deriving a mantle reference frame that isolates the plate–mantle system for geodynamic and mantle flow modeling. We derive a new absolute reference frame using the optimization approach of Tetley et al. (2019) as presented in the study by Müller et al. (2019).

From 400–180 Ma, kinematics of terranes on the western North American margin (Alexander, Stikinia, Yukon-Tanana and Klamath terranes) were modified to improve the relative plate motions implied by the plate boundaries (i.e., convergence across subduction zones). First, the back-arc seafloor spreading history of the Alexander Terrane between 375 and 315 Ma was revised to be more consistent with the plate boundary evolution. A westward ridge jump is implemented at 315 Ma to ensure the self-consistency of the regional plate kinematics. Second, the back-arc basin seafloor spreading history representing the Slide Mountain Ocean (related to the Stikinia–Yukon-Tanana terranes) was improved so that the synthetic isochrons and fracture zones follow the small circles of relative plate motions between 340 and 270 Ma, followed by a subduction polarity reversal to consume the back-arc basin seafloor at a west-dipping intra-oceanic subduction system.

2.2 | Evolving model of carbonate platforms and subduction zone interactions

Arc volcanism results from the release of volatiles (H_2O , CO_2 , and SO_2 , followed by H_2S , HCl , HF , H_2 , CO , N_2 , Ar , and He) (Edmonds & Wallace, 2017; Fischer, 2008) from the slab in the mantle wedge, with the location of

volcanism on the overriding plate determined to an extent by the slab dip. Predicting the precise arc interactions with (buried) carbonate platforms in deep time is difficult because of the complex relationship between oceanic crust

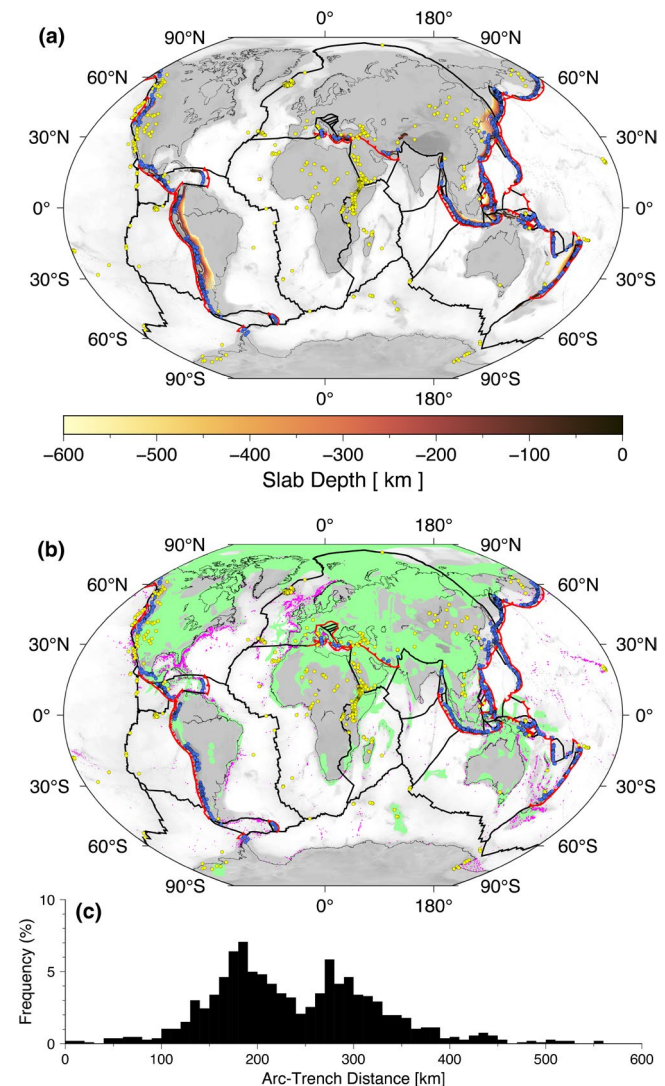


FIGURE 1 Distance between volcanoes and the subduction zone trench locations at present-day is used to infer the typical range of volcanic arc distances from active margins and their interactions with buried carbonate platforms. (a) Subduction zones and their polarities are plotted as red lines with triangles on the overriding plate, and volcanoes from the Smithsonian Institution's Global Volcanism Program (Venzke, 2013) are plotted as blue (subduction-related) and yellow (non-subduction-related) circles. Slab depth contours from SLAB2 (Hayes et al., 2018) are plotted to provide an insight into volcanic arc locations and slab dips. (b) Interaction between arc volcanoes and (buried) carbonate platforms has been shown to increase CO_2 liberation from carbonate rocks. Present-day cool- and warm-water reefs (UNEP-WCMC, 2018) in magenta and ancient carbonate platform systems are in light green (Kiessling et al., 2003; Pall et al., 2018). (c) Present-day distance histogram between subduction-related volcanoes and subduction zones (see Supporting Information 1.1)

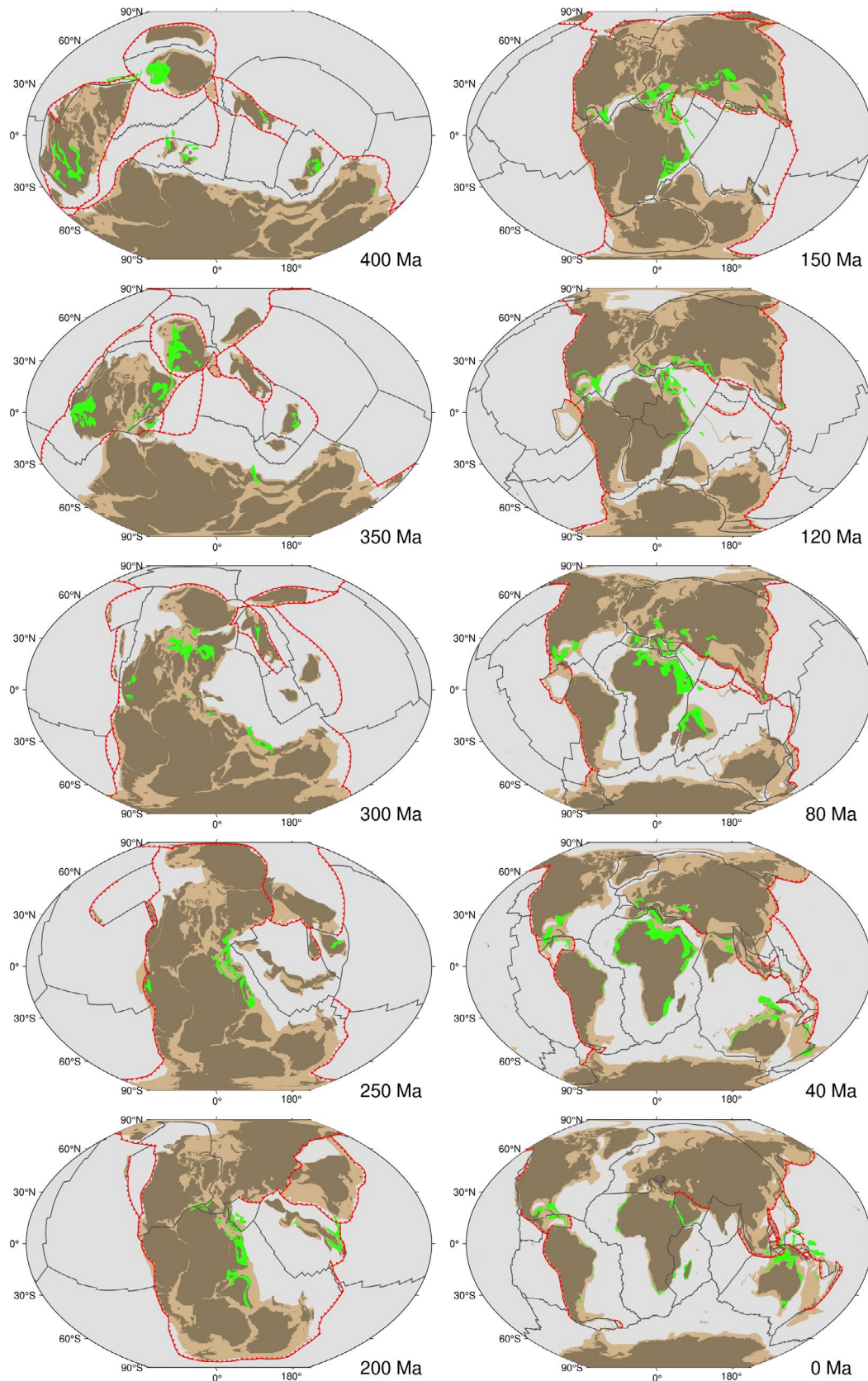


FIGURE 2 Reconstructions of active carbonate platforms (green) in the study by Matthews et al. (2016) as adapted from Kiessling et al. (2003) and presented by Pall et al. (2018) and updated in this study. The interaction between subduction zones (teethed lines) and carbonate platforms within 436 km away from the trenches, in the overriding plate, is tracked through time in the workflow presented here. Light beige areas represent continental crust extents, while dark beige regions are reconstructed present-day coastlines

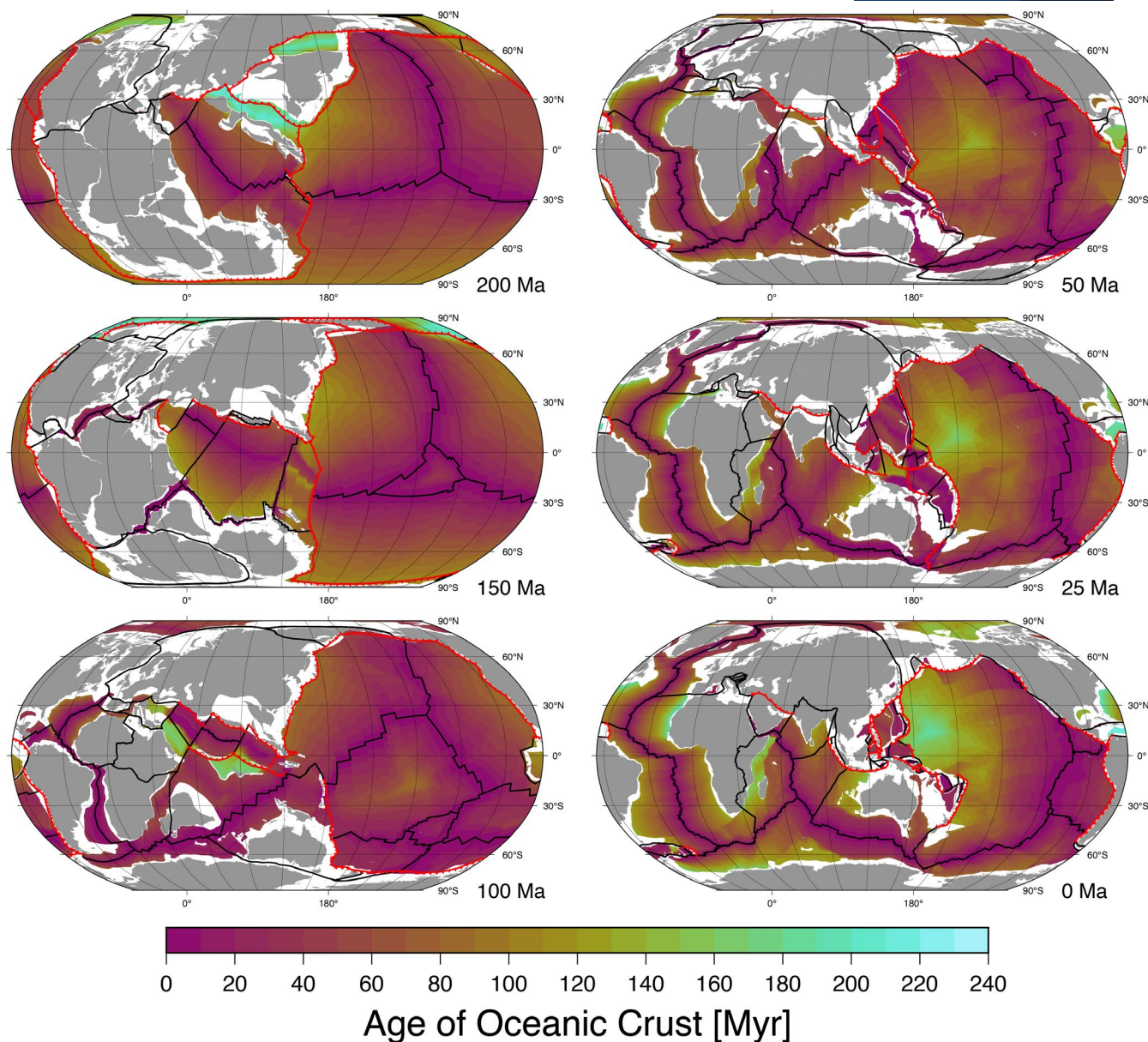


FIGURE 3 Time-evolving distribution of oceanic crustal age in the last 200 Myr from the Matthews et al. (2016) plate motion model. Gray regions are reconstructed present-day terranes/coastlines, black lines indicate mid-oceanic ridge or transform plate boundaries, and teethed red lines indicate subduction zones

age, plate kinematics, and slab dip (Cruciani et al., 2005; Lallemand et al., 2005). Instead, we measure the range of distances between arc volcanoes and subduction zone trenches at the present-day (Figure 1), with most (~84%) arc volcanoes occurring within 436 km from the trenches on the overriding plate (Supporting Information 1.1).

Subduction zone geometries, and their polarity, are extracted from time-evolving plate topologies using pyGPlates. First, global subduction zone lengths are computed by removing duplicate or overlapping subduction zone geometries (Supporting Information 1.2). Second, the subduction zone lengths interacting with carbonate platforms to a maximum distance of 436 km from the trench on the

overriding plate are extracted using Generic Mapping Tools (Wessel et al., 2019) (Supporting Information 1.3).

The carbonate platform maps from Kiessling et al. (2003) were georeferenced and reprojected into geographic coordinates, and using GPlates, the geometries were forward-rotated into present-day geometries – allowing the platforms to be connected to any plate tectonic reconstruction (Figure 2) (Supporting Information 1.3). Given that carbonate platforms tend to accumulate on continental margins, and are also ‘consumed’ in decarbonation processes during arc volcanism, it is difficult to know how much a carbonate platform is eroded, buried, or consumed during volcanism and tectonism. We present

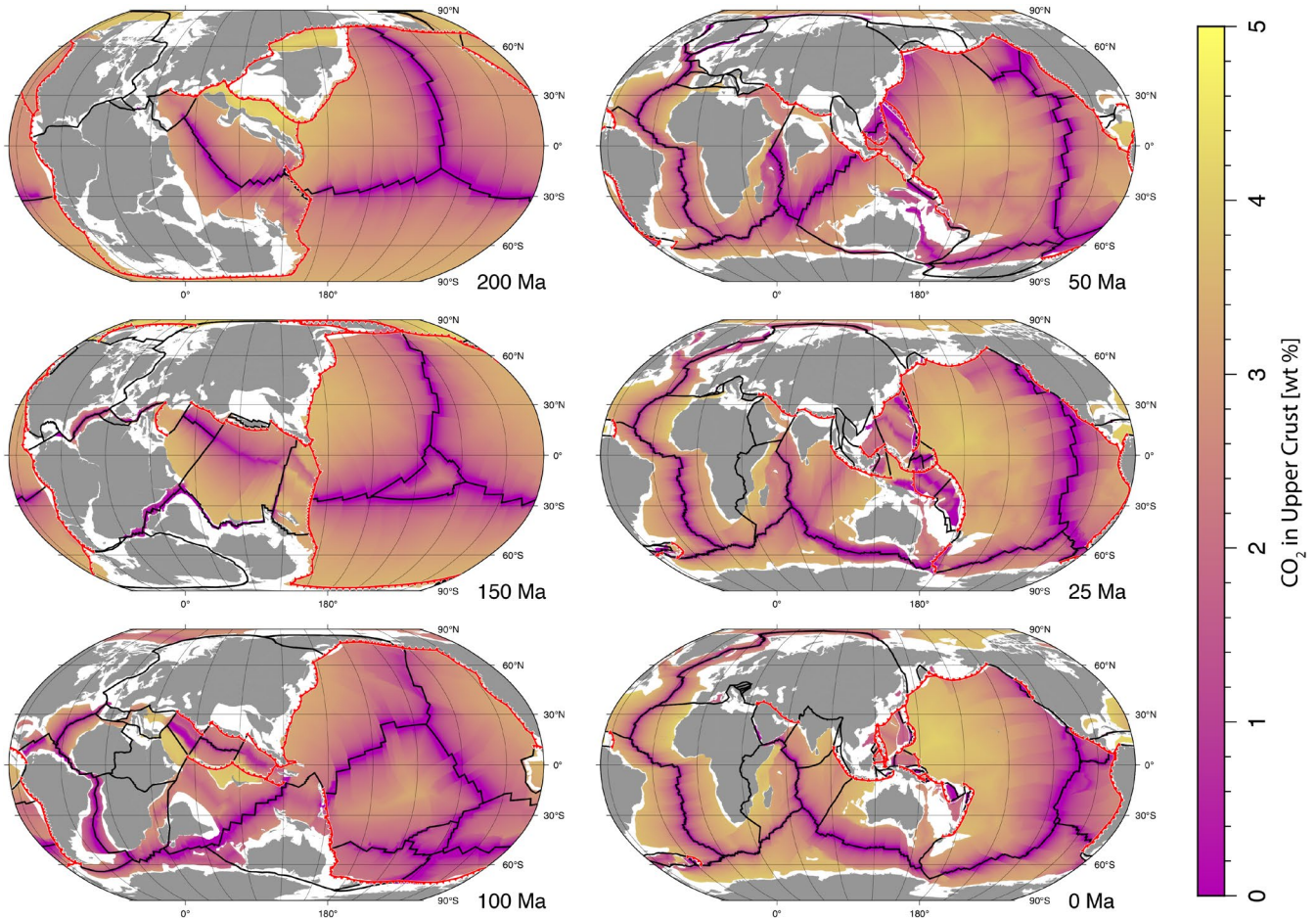


FIGURE 4 Estimated CO_2 (wt. %) content in the oceanic upper crust following Jarrard (2003), derived from the oceanic crustal age in the Matthews et al. (2016) model. Gray regions are reconstructed present-day terranes/coastlines, black lines indicate mid-oceanic ridge or transform plate boundaries, and teethed red lines indicate subduction zones

a conservative end-member where only actively growing major reefs and carbonate platforms are considered in the analysis. Future research will be required to estimate the thicknesses and carbon contents of these crustal features to better evaluate the CO_2 degassing potential during magmatic interactions.

2.3 | Oceanic crust CO_2 content and seafloor sediment thickness

Oceanic crustal age is an inherent component of a plate reconstruction model such as the one by Matthews et al. (2016), and is used to ‘undo’ seafloor spreading in order to restore the Pangea supercontinental arrangement. Oceanic crustal age, particularly through time, can be used to estimate sediment thickness (Anderson & Hobart, 1976; Bird & Pockalny, 1994; Dutkiewicz et al., 2017), CO_2 crustal content (Jarrard, 2003), and other parameters, largely driven by the progressive ageing of oceanic crust away from the mid-oceanic ridge. As the Matthews et al.

(2016) model was not released with a seafloor age-grid, we updated the seafloor spreading history and computed seafloor age-grids in 1 Myr intervals for 200 to 0 Ma (Figure 3). The updates to the Matthews et al. (2016) model presented here also include corrections to the Pacific Plate motions following Torsvik et al. (2019).

To estimate the total amount of carbon being subducted at a given time step and at 0.1° great circle intervals along the subduction zone, orthogonal convergence velocities (cm/yr) were combined with CO_2 (wt. %), assuming that CO_2 (wt. %) estimates of Jarrard (2003) apply only to the upper 300 m of the oceanic crust where hydrothermal alteration is greatest (Gillis & Coogan, 2011) (Figure 4). We follow the approach of Muller and Dutkiewicz (2018), but do not consider the role of bottom-water temperature in hydrothermal reactions. We compute the area of the subducting plate using the East et al. (2020) workflow, apply the 300-m thickness of the upper oceanic crust layer, and compute the volume of the subducting uppermost oceanic crust. The volume is converted to a weight of basalt with a density of

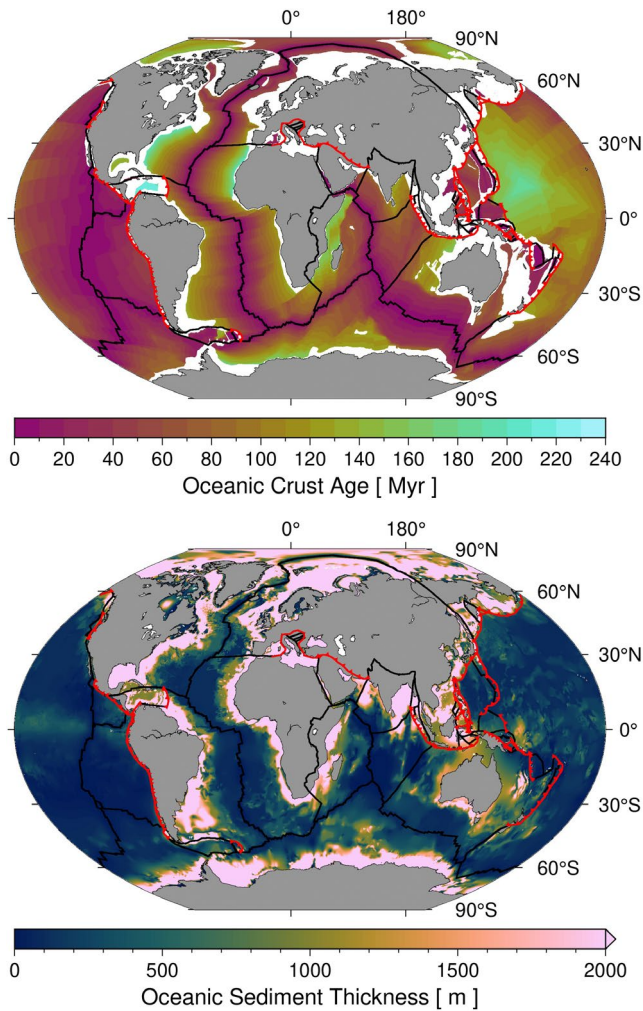


FIGURE 5 (a) Present-day oceanic crust age from the plate reconstruction of the Matthews et al. (2016). (b) Oceanic sediment thickness from GlobSed-v2 (Straume et al., 2019). Gray regions are present-day emergent continental regions, black lines indicate mid-oceanic ridge or transform plate boundaries, and teethed red lines indicate subduction zones

2,900 kg/m³, and the weight of carbon is computed from CO₂ (wt. %) (Supporting Information 2.1).

A relationship between seafloor age and passive margin distance from the Matthews et al. (2016) model and the sediment thickness from the Straume et al. (2019) model was derived at the present day (Figure 5, Figure S3) following the technique in the study by Dutkiewicz et al. (2017). Thirteen major river mouth regions were excluded from the analysis as they would bias the oceanic crust age-sediment thickness relationship, also following Dutkiewicz et al. (2017). The workflow was updated to use a global spherical icosahedral sampling mesh with an approximate mesh node spacing of 150 km using Stripy (Moresi & Mather, 2019) (Supporting Information 2.2). Sediment thickness estimates were computed only back to 200 Ma (Figure 6)

as this is the period where pelagic marine calcifiers contributed significant amounts of sediments to the seafloor (Hull, 2017).

The sediment thicknesses arriving at subduction zones were combined with the orthogonal plate convergence rates using an updated variant of the East et al. (2020) approach using pyGPlates rev. 28 and Python 3, which now also enables the interrogation of plate reconstructions that include deformation (e.g., Müller et al., 2019). This enabled the comparison of subduction zone (and implied volcanic arc) lengths (Figure 7) with the subducting plate area and predicted subducting volumes of sediments (Figure 8).

2.4 | Data and model reproducibility

The most recent version of the toolkit, and related data, described here can be accessed from <https://github.com/sabinz/DCO-Modelling-of-Deep-Time-Atmospheric-Carbon-Flux-from-Subduction-Zone-Interactions>. The workflows presented here work best in Unix-like environments such as Linux (including in virtual machines), macOS, or the Windows Subsystem for Linux available since Windows 10. Currently, pyGPlates (revision 28 or more recent; www.gplates.org) requires Python 3. The open-source Generic Mapping Tools (GMT 6.2, www.generic-mapping-tools.org) are used for geospatial data processing and visualization (Wessel et al., 2019). Full digital supplement (~15 Gb), including the workflows, input grids, plate motion model, time series, and animation, is available from Zenodo repository accessible from <https://zenodo.org/record/4729046>.

3 | RESULTS AND DISCUSSIONS

Global total subduction zone lengths have fluctuated since the Devonian, reaching almost 100,000 km at ~260 Ma, followed by lows of ~60,000 km at ~240 and 140 Ma (Figure 7a) in the Matthews et al. (2016) plate reconstruction. By comparison, the peak in subduction zone lengths of ~75,000 km occurs at ~330–320 Ma in the hybrid alternative model that we present here (Z2021-MCY). Unsurprisingly, the pre-Pangea (pre-250 Ma) time-frame shows greater uncertainty and disagreement in the Paleozoic reconstructions in the Domeier and Torsvik (2014) model that are adopted and modified in Matthews et al. (2016), while the Young et al. (2018) Paleozoic reconstructions are incorporated in the hybrid Z2021-MCY model presented here.

More directly pertinent to the deep carbon cycle, the interaction of subduction zone magmatism and carbonate

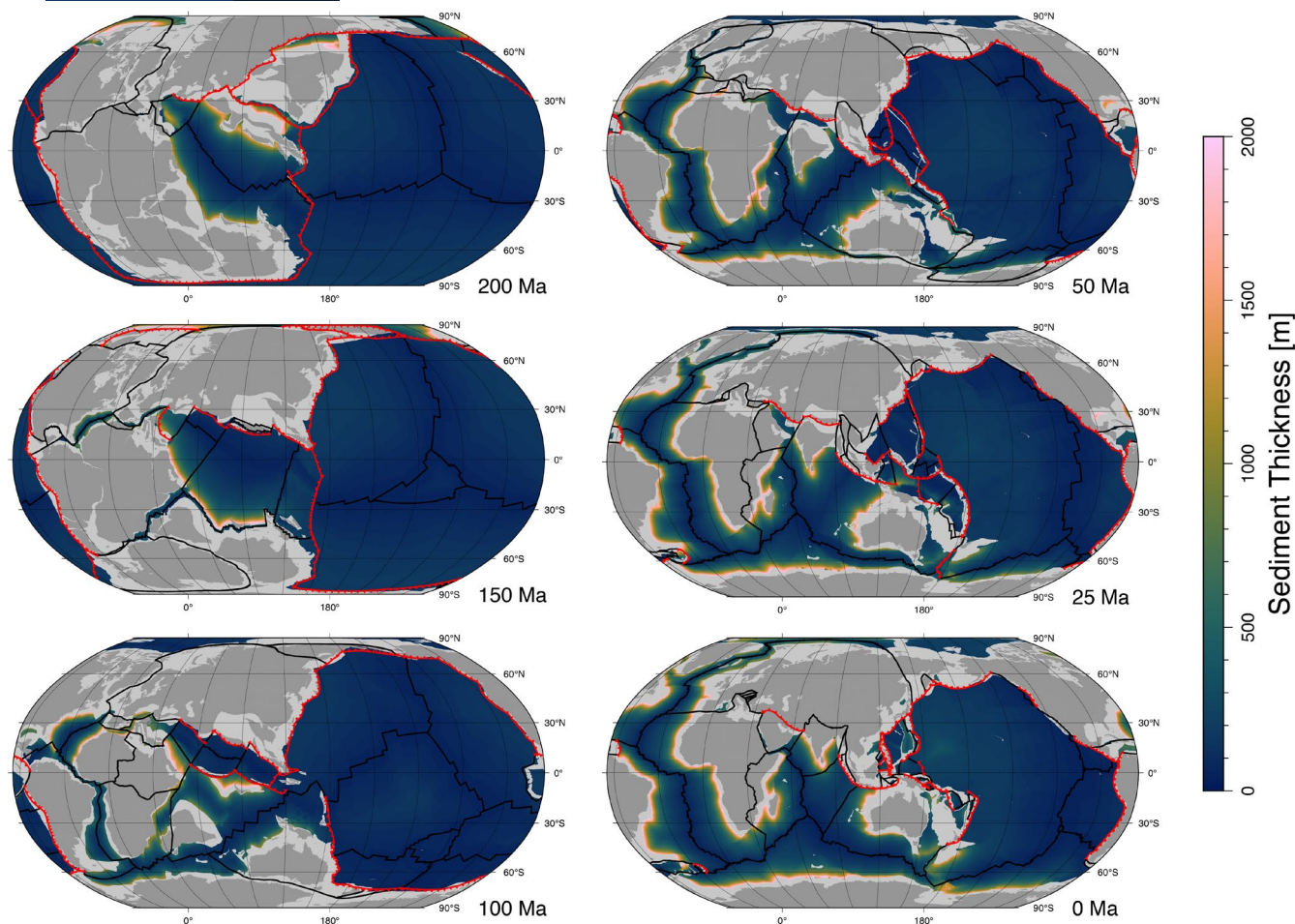


FIGURE 6 Estimated evolution of oceanic crust sediment thicknesses over the last 200 Myr using the Matthews et al. (2016) plate reconstruction model. Gray regions are reconstructed present-day terranes/coastlines, black lines indicate mid-oceanic ridge or transform plate boundaries, and teethed red lines indicate subduction zones

platforms in the overriding plate is a critical process for liberating CO_2 from the (buried) limestone. The results presented here are conservative as we analyze only the presence of actively accumulating carbonate platforms in the overriding plate above a subducting slab (Figure 7b). This process appears to be at a minimum (0 to 1000 km) during the Pangea supercontinent timeframe (~ 300 – 250 Ma), but steadily increases to $\sim 5,000$ km of subduction zone lengths interacting with carbonate platforms between ~ 170 and 120 Ma, and peaks by ~ 100 Ma to totals of $\sim 10,000$ km. As we do not consider the role of inactive buried carbonate platforms, nor the variable thickness of carbonate platform accumulations, our estimates are likely to represent a minimum. However, they do provide some interesting insights, including the relatively elevated values of carbonate platform–subduction interactions during the Cretaceous greenhouse climate, the increase between ~ 80 and 50 Ma during Tethyan subduction and oceanic gateway closures, as well as the more recent (~ 15 – 5 Ma) subduction–carbonate platform interactions in the Mediterranean, Southeast Asia, and central Americas.

Continental arc lengths in the plate reconstructions are at a minimum in the Pangea assembly phase (~ 380 – 320 Ma) with values of $\sim 10,000$ – $20,000$ km, increasing to $\sim 25,000$ – $40,000$ km by 320 Ma (Figure 7c). Continental arc lengths fluctuate between $\sim 35,000$ to $50,000$ km between 150 Ma and the present; however, some of these higher recent values may be amplifying the problem of retro-deforming and accurately reconstructing the past shape of continental blocks in deeper time. The proportion of subduction zones that interact with the overriding continental crust, such as Andean-style subduction systems, show an increasing trend during these supercontinent final assembly and early breakup phases. This estimate grows from a value of $\sim 20\%$ – 50% at ~ 400 Ma to $\sim 60\%$ – 80% by 150 Ma (Figure 7d). However, the size of continents in the Paleozoic (pre 250 Ma) is more difficult to constrain as many have been deformed and shortened during Pangea assembly, with a small portion having been potentially lost to subduction, meaning that our continental arc length portions of the global subduction system are conservative in the pre-Pangea timeframes. Overall, the

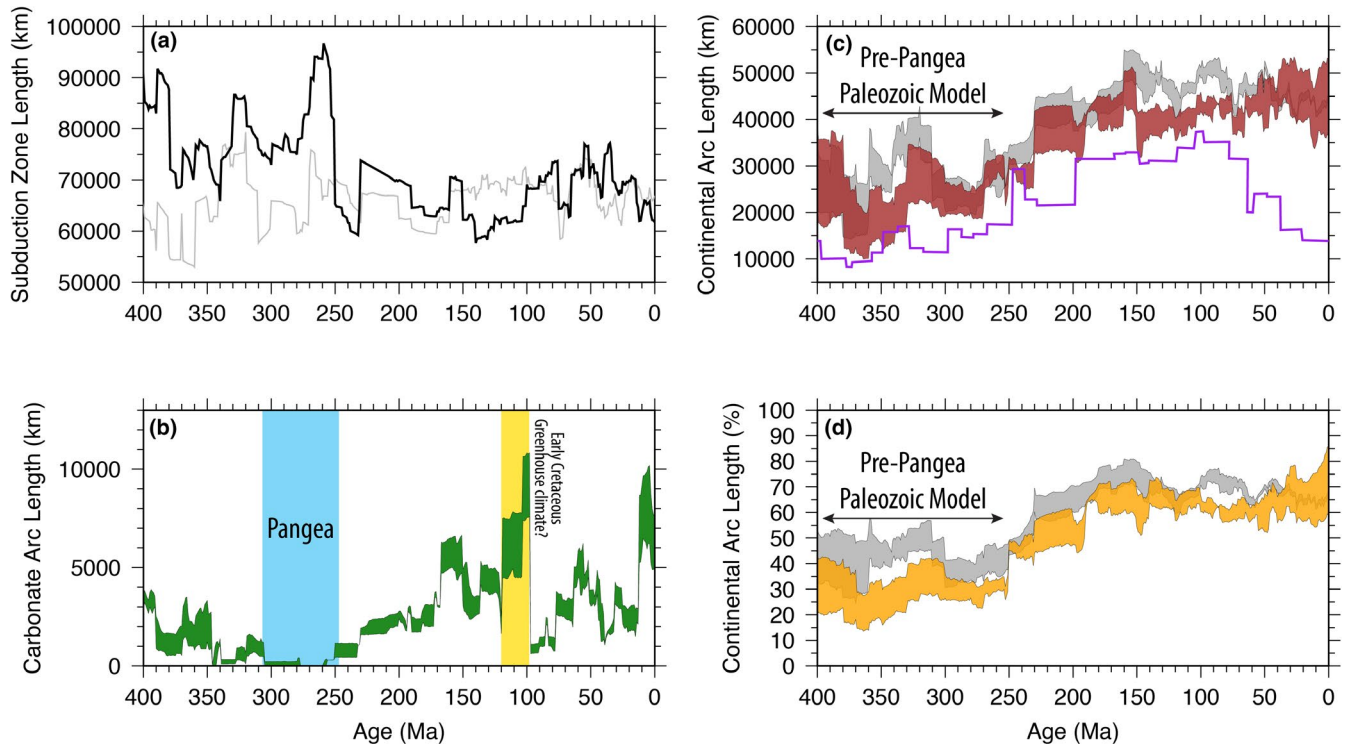


FIGURE 7 (a) Subduction zone lengths in the Matthews et al. (2016) model [black], and for comparison, subduction zone lengths in the hybrid model presented in this article (Model Z2021-MCY) [grey]. (b) Carbonate platform interactions with subduction zones in the Matthews et al. (2016) model [green] are plotted using a range of arc-trench distances from 254 km (mean) to 436 km (mean + 1SD). (c) Continental arc lengths in the Matthews et al. (2016) model [maroon], and for comparison, continental arc lengths in the hybrid model presented in this article (Model Z2021-MCY) [gray], with the uncertainty derived from assuming arc-trench distances of 254 km (mean) to 436 km (mean + 1SD). The mean continental arc lengths from Cao et al. (2017) are presented for comparison [purple]. (d) Continental arc length portions (%) of the global subduction zone lengths. Continental arc lengths, and also intra-oceanic arc lengths, are more uncertain pre 250 Ma (pre-Pangea) times due to the difficulty in capturing continental deformation and the difficulty in reconstructing intra-oceanic subduction systems (particularly in the proto Pacific)

analysis provides a first-order estimate for the relative influence of Andean-style versus intra-oceanic subduction since the Devonian.

Arc volcanism is at least partially controlled by volatiles, such as water and carbon, entering the subduction system. As a result, a key constraint of volatile input into the trench comes from quantifying the subducting plate area (East et al., 2020) over time. The three plate reconstructions presented here show similar trends in the subducting plate area for the post-Pangea timeframe, with a significant peak between ~160 and 120 Ma (Figure 8a). This peak was previously discussed by East et al. (2020), implicated in strengthening mantle return flow to produce the Darwin Rise in the Pacific (McNutt et al., 1990), and potentially triggering the eruption of the Ontong–Java–Manihiki–Hikurangi super-Large Igneous Province at ~123 Ma (Ernst & Buchan, 2002) and other LIP eruptions in the mid to Late Cretaceous (East et al., 2020). This pulse in subduction also corresponds with elevated volumes of sediment (Figure 8b) and carbon (Figure 8c) being subducted, and may explain the shift to a greenhouse climate

in the mid Cretaceous (Figure 8b), as well as the magma flare-up events recorded in continental arcs (Ratschbacher et al., 2019) (Figure 8b).

Ongoing efforts are focused on improving the plate tectonic reconstructions, particularly where the seafloor spreading history has been lost. For example, the oldest reliably-dated seafloor spreading occurred from ~190 Ma in the equatorial Atlantic during Pangea breakup, while the earliest portions of the Pacific Plate only formed from ~170 Ma (Müller et al., 2019). Although paleomagnetic data collection and compilations have tremendously improved our understanding of pre-Pangea continental arrangements, emerging data and interpretations require major re-evaluations of fundamental assumptions of Pangea assembly scenarios (e.g., Wu et al., 2021), which also impacts the tectonic evolution of central and east Asia, as well as the trajectory of Tethyan terranes toward Eurasia.

The workflow presented here is the first step toward creating quantifiable links between tectonics and the planetary carbon cycle. For example, it remains difficult

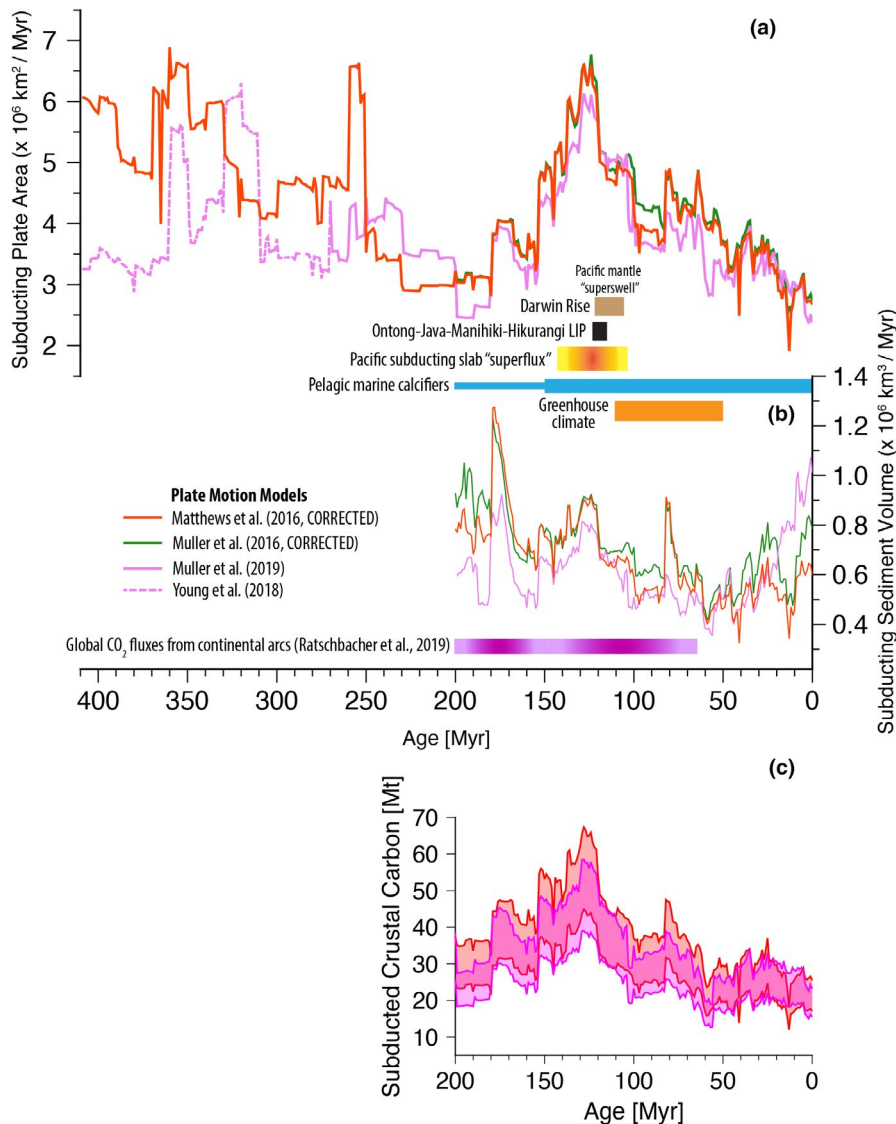


FIGURE 8 (a) Subducting plate area from the Devonian to present as implied by the Matthews et al. (2016) and Müller et al. (2016) plate reconstructions with corrections to Pacific plate motions (Torsvik et al., 2019), as well as the Müller et al. (2019) and Young et al. (2018) plate motions. (b) Estimated subducting sediment thickness volumes from the different plate motion models during the time where pelagic marine calcifiers were contributing to sediment accumulation on the seafloor. Periods of continental volcanic arc “flare-ups” may be linked to high rates of the subducting plate area and/or high rates of sediment subduction, driving water, and/or carbon volatiles into the mantle wedge. (c) Estimated subducted carbon in the upper 300 m of the oceanic crust using the Müller et al. (2019) [magenta] and Matthews et al. (2016) corrected reconstructions [red]. The minimum value represents the contribution from the upper oceanic crust (i.e., two thirds of the total contribution), and the upper value represents the estimated total contribution from the oceanic crust

to estimate the time-evolving volatile content and sediment thickness on the oceanic crust (Dutkiewicz et al., 2018; Merdith et al., 2019), considering that only small parcels of seafloor are drilled to reach the basement (Jarrard, 2003). In addition, it remains difficult to constrain the balance of inputs and outputs in a subduction system – namely, how much carbon is subducted (as opposed to scraped off in the accretionary prism), how much of the subducted carbon is returned to the atmosphere through arc volcanism, how much is trapped in lithospheric reservoirs, and how much may be returned to the convecting mantle (Dasgupta & Hirschmann, 2010; Kelemen & Manning, 2015). More broadly, these workflows can also be adapted to consider the planetary water cycle on geological timescales, which has received renewed interest in recent times (e.g., Karlsen et al., 2019; Merdith et al., 2019). However, incorporating the components of the deep carbon cycle presented here, while also capturing other geological sources and

sinks, such as the role of Large Igneous Provinces (Jones et al., 2019), silicate weathering (Brady, 1991), and metamorphic degassing in orogens (Kerrick & Caldeira, 1993, 1998) will form a key input for carbon box models and our broader understanding of carbon cycle and climate perturbations in deep time.

4 | CONCLUSION

We have presented an open-source toolkit for the analysis of subduction zone kinematics and interactions between active margins and carbonate platforms over the past 410 million years. For more recent times, where seafloor spreading histories are preserved, subducted volumes of oceanic sediment thicknesses and carbon contributions from the oceanic upper crust are estimated for the last 200 million years during Pangea breakup. The plate reconstructions with evolving plate topologies compared

in this study suggest a significant perturbation to planetary carbon cycling and climate in the Early Cretaceous and suggest that the mid-Cretaceous greenhouse climate was driven by tectonic remobilization of carbon into the atmosphere. The subduction of Tethyan ocean basins in the Late Cretaceous likely led to significant decarbonation of carbonate platforms that were forming on the Tethyan passive margins (e.g., Greater India). These examples highlight the need for future work to quantify carbonate platform thicknesses (and carbon contents), as well as the relative contributions of these carbon reservoirs and fluxes in driving long-term climate change. Importantly, the tools presented here enable the interrogation of digital plate motion models built in GPlates, and the results provide crucial insights into the planetary carbon cycle, deep-time climate, and could even aid frontier exploration of skarn ore deposits that are formed from the interactions between limestone and volcanism.

ACKNOWLEDGEMENTS

We thank Nicky Wright for helpful discussions on the deep-time estimation of sediment thicknesses. We thank Maria Seton for publicly releasing the Matthews et al. (2016) and the Müller et al. (2016) models that included fixes to Pacific plate motions flagged by Torsvik et al. (2019). We thank Douwe van Hinsbergen, Richard Palin, and an anonymous reviewer for feedback that improved the manuscript. SZ was supported by the Australian Research Council grant DE210100084 and a University of Sydney Robinson Fellowship. JP, SD, and SZ were supported by Alfred P Sloan grants G-2017-9997 and G-2018-11296. MP was supported by Ambizione Fellowship (grant PZ00P2_168166) of the Swiss National Science Foundation and UGA Presidential Funds. MGT was supported by the AUGURY European Research Council (ERC) Project 617588. pyGPlates and GPlates development is funded by the AuScope National Collaborative Research Infrastructure System (NCRIS) program from the Australian government. The authors have no conflicts of interest to declare. This manuscript is dedicated to the memory of Peter Fox.

AUTHOR CONTRIBUTIONS

Sabin Zahirovic: Conceptualization (equal); Data curation (lead); Formal analysis (lead); Funding acquisition (lead); Investigation (lead); Methodology (lead); Project administration (lead); Resources (equal); Software (equal); Supervision (lead); Validation (lead); Visualization (lead); Writing – original draft (lead); Writing – review & editing (lead). **Ahmed Eleish:** Investigation (supporting); Methodology (supporting); Project administration (supporting); Software (equal); Validation (lead); Writing – original draft (equal); Writing – review & editing (equal). **Jodie Pall:** Data curation (lead); Formal analysis (equal);

Investigation (equal); Methodology (equal); Resources (lead); Software (lead); Validation (equal); Visualization (equal); Writing – review & editing (equal). **Sebastiano Doss:** Data curation (equal); Formal analysis (equal); Investigation (equal); Methodology (equal); Resources (equal); Software (lead); Validation (equal); Visualization (equal); Writing – review & editing (equal). **John Cannon:** Software (equal); Validation (equal); Writing – review & editing (equal). **Mattia Pistone:** Validation (lead); Writing – review & editing (equal). **Michael Grant Tetley:** Software (equal); Validation (equal); Writing – review & editing (equal). **Alexander Young:** Methodology (supporting); Software (equal); Validation (supporting); Writing – review & editing (equal). **Peter Fox:** Investigation (supporting); Project administration (supporting); Supervision (equal); Writing – review & editing (equal).

OPEN PRACTICES STATEMENT

This article has earned an Open Data badge for making publicly available the digitally shareable data necessary to reproduce the reported results. The data is available at [HYPERLINK “https://urldefense.com/v3/__https://zenodo.org/record/4729046__!!N11eV2iwtfslvck8mED9fvm7Vh80nqrsX6RLWDUk5Pp5NXYvJcQzNmYfGfNYolGv3Q2E1SZ7jMh_CTH64fQYJ3B8rNtSFd0SDzxAS5AW0v8U\\$”](https://urldefense.com/v3/__https://zenodo.org/record/4729046__!!N11eV2iwtfslvck8mED9fvm7Vh80nqrsX6RLWDUk5Pp5NXYvJcQzNmYfGfNYolGv3Q2E1SZ7jMh_CTH64fQYJ3B8rNtSFd0SDzxAS5AW0v8U$) <https://zenodo.org/record/4729046>. Learn more about the Open Practices badges from the Center for Open Science: <https://osf.io/tyvxyz/wiki>.

ORCID

Sabin Zahirovic  <https://orcid.org/0000-0002-6751-4976>

Mattia Pistone  <https://orcid.org/0000-0001-7560-3146>

Michael G. Tetley  <https://orcid.org/0000-0002-2320-4239>

REFERENCES

- Anderson, R.N. & Hobart, M.A. (1976) The relation between heat flow, sediment thickness, and age in the eastern Pacific. *Journal of Geophysical Research*, 81(17), 2968–2989. Available at: <https://doi.org/10.1029/JB081i017p02968>
- Bird, R.T. & Pockalny, R.A. (1994) Late Cretaceous and Cenozoic seafloor and oceanic basement roughness: Spreading rate, crustal age and sediment thickness correlations. *Earth and Planetary Science Letters*, 123(1–3), 239–254. Available at: [https://doi.org/10.1016/0012-821X\(94\)90271-2](https://doi.org/10.1016/0012-821X(94)90271-2)
- Brady, P.V. (1991) The effect of silicate weathering on global temperature and atmospheric CO₂. *Journal of Geophysical Research: Solid Earth*, 96(B11), 18101–18106.
- Cao, W., Lee, C.-T.-A. & Lackey, J.S. (2017) Episodic nature of continental arc activity since 750 Ma: a global compilation. *Earth and Planetary Science Letters*, 461, 85–95. Available at: <https://doi.org/10.1016/j.epsl.2016.12.044>
- Cao, X., Zahirovic, S., Li, S., Suo, Y., Wang, P., Liu, J. et al. (2020) A deforming plate tectonic model of the South China Block since

- the Jurassic. *Gondwana Research*. <https://doi.org/10.1016/j.gr.2020.11.010>
- Cruciani, C., Carminati, E. & Doglioni, C. (2005) Slab dip vs. lithosphere age: no direct function. *Earth and Planetary Science Letters*, 238(3–4), 298–310. Available at: <https://doi.org/10.1016/j.epsl.2005.07.025>
- Dasgupta, R. & Hirschmann, M.M. (2010) The deep carbon cycle and melting in Earth's interior. *Earth and Planetary Science Letters*, 298(1–2), 1–13. Available at: <https://doi.org/10.1016/j.epsl.2010.06.039>
- Domeier, M. & Torsvik, T.H. (2014) Plate tectonics in the late Paleozoic. *Geoscience Frontiers*, 5(3), 303–350. Available at: <https://doi.org/10.1016/j.gsf.2014.01.002>
- Dutkiewicz, A., Müller, R.D., Cannon, J., Vaughan, S. & Zahirovic, S. (2018) Sequestration and subduction of deep-sea carbonate in the global ocean since the Early Cretaceous. *Geology*, 47(1), 91–94. Available at: <https://doi.org/10.1130/G45424.1>
- Dutkiewicz, A., Müller, R., Wang, X., O'Callaghan, S., Cannon, J. & Wright, N. (2017) Predicting sediment thickness on vanished ocean crust since 200 ma. *Geochemistry, Geophysics, Geosystems*, 18(12), 4586–4603. Available at: <https://doi.org/10.1002/2017GC007258>
- East, M., Müller, R.D., Williams, S.E., Zahirovic, S. & Heine, C. (2020) Subduction history reveals Cretaceous slab superflux as a possible cause for the mid-Cretaceous plume pulse and superswell events. *Gondwana Research*, 79, 125–139. Available at: <https://doi.org/10.1016/j.gr.2019.09.001>
- Edmonds, M. & Wallace, P.J. (2017) Volatiles and exsolved vapor in volcanic systems. *Elements*, 13(1), 29–34. Available at: <https://doi.org/10.2113/gselements.13.1.29>
- Ernst, R.E. & Buchan, K.L. (2002) Maximum size and distribution in time and space of mantle plumes: evidence from large igneous provinces. *Journal of Geodynamics*, 34(2), 309–342. Available at: [https://doi.org/10.1016/S0264-3707\(02\)00025-X](https://doi.org/10.1016/S0264-3707(02)00025-X)
- Fischer, T.P. (2008) Fluxes of volatiles (H₂O, CO₂, N₂, Cl, F) from arc volcanoes. *Geochemical Journal*, 42(1), 21–38. Available at: <https://doi.org/10.2343/geochemj.42.21>
- Gillis, K. & Coogan, L. (2011) Secular variation in carbon uptake into the ocean crust. *Earth and Planetary Science Letters*, 302(3–4), 385–392. Available at: <https://doi.org/10.1016/j.epsl.2010.12.030>
- Gurnis, M., Yang, T., Cannon, J., Turner, M., Williams, S., Flament, N. et al. (2018) Global tectonic reconstructions with continuously deforming and evolving rigid plates. *Computers & Geosciences*, 116, 32–41. Available at: <https://doi.org/10.1016/j.cageo.2018.04.007>
- Hayes, G.P., Moore, G.L., Portner, D.E., Hearne, M., Flamme, H., Furtney, M. et al. (2018) Slab2, a comprehensive subduction zone geometry model. *Science*, 362(6410), 58–61. Available at: <https://doi.org/10.1126/science.aat4723>
- Hull, P.M. (2017) Emergence of modern marine ecosystems. *Current Biology*, 27(11), R466–R469. Available at: <https://doi.org/10.1016/j.cub.2017.04.041>
- Isson, T.T., Planavsky, N.J., Coogan, L.A., Stewart, E.M., Ague, J.J., Bolton, E.W. et al. (2020) Evolution of the global carbon cycle and climate regulation on earth. *Global Biogeochemical Cycles*, 34(2), e2018GB006061.
- Jarrard, R.D. (2003) Subduction fluxes of water, carbon dioxide, chlorine, and potassium. *Geochemistry, Geophysics, Geosystems*, 4(5), 1–50.
- Johansson, L., Zahirovic, S. & Müller, R.D. (2018) The interplay between the eruption and weathering of large igneous provinces and the deep-time carbon cycle. *Geophysical Research Letters*, 45(11), 5380–5389. Available at: <https://doi.org/10.1029/2017GL076691>
- Jones, S.M., Hoggett, M., Greene, S.E. & Jones, T.D. (2019) Large igneous province thermogenic greenhouse gas flux could have initiated paleocene-eocene thermal maximum climate change. *Nature Communications*, 10(1), 1–16.
- Karlsen, K.S., Conrad, C.P. & Magni, V. (2019) Deep water cycling and sea level change since the breakup of Pangea. *Geochemistry, Geophysics, Geosystems*, 20(6), 2919–2935. Available at: <https://doi.org/10.1029/2019GC008232>
- Kelemen, P.B. & Manning, C.E. (2015) Reevaluating carbon fluxes in subduction zones, what goes down, mostly comes up. *Proceedings of the National Academy of Sciences*, 112(30), E3997–E4006. Available at: <https://doi.org/10.1073/pnas.1507889112>
- Kerrick, D. & Caldeira, K. (1993) Paleoatmospheric consequences of CO₂ released during early Cenozoic regional metamorphism in the Tethyan orogen. *Chemical Geology*, 108(1–4), 201–230. Available at: [https://doi.org/10.1016/0009-2541\(93\)90325-D](https://doi.org/10.1016/0009-2541(93)90325-D)
- Kerrick, D.M. & Caldeira, K. (1998) Metamorphic CO₂ degassing from orogenic belts. *Chemical Geology*, 145(3–4), 213–232. Available at: [https://doi.org/10.1016/S0009-2541\(97\)00144-7](https://doi.org/10.1016/S0009-2541(97)00144-7)
- Kiessling, W., Flügel, E. & Golonka, J. (2003) Patterns of Phanerozoic carbonate platform sedimentation. *Lethaia*, 36(3), 195–225. Available at: <https://doi.org/10.1080/00241160310004648>
- Lallemand, S., Heuret, A. & Boutelier, D. (2005) On the relationships between slab dip, back-arc stress, upper plate absolute motion, and crustal nature in subduction zones. *Geochemistry, Geophysics, Geosystems*, 6(9), 1–18.
- Lee, C.-T.-A., Jiang, H., Dasgupta, R. & Torres, M. (2019). A framework for understanding whole-earth carbon cycling. In: Orcutt, B.N., Daniel, I. & Dasgupta, R. (Eds.) *Deep Carbon: Past to Present*. Cambridge: Cambridge University Press, pp. 313–357.
- Liu, S., Gurnis, M., Ma, P. & Zhang, B. (2017) Reconstruction of northeast Asian deformation integrated with western Pacific plate subduction since 200Ma. *Earth-science Reviews*, 175, 114–142. Available at: <https://doi.org/10.1016/j.earscirev.2017.10.012>
- Matthews, K.J., Maloney, K.T., Zahirovic, S., Williams, S.E., Seton, M. & Müller, R.D. (2016) Global plate boundary evolution and kinematics since the late Paleozoic. *Global and Planetary Change*, 146, 226–250. Available at: <https://doi.org/10.1016/j.gloplacha.2016.10.002>
- McNutt, M., Winterer, E., Sager, W., Natland, J. & Ito, G. (1990) The Darwin rise: a Cretaceous superswell? *Geophysical Research Letters*, 17(8), 1101–1104. Available at: <https://doi.org/10.1029/GL017i008p01101>
- Merdith, A.S., Atkins, S.E. & Tetley, M.G. (2019) Tectonic controls on carbon and serpentinite storage in subducted upper oceanic lithosphere for the past 320 ma. *Frontiers in Earth Science*, 7, 332.
- Moresi, L. & Mather, B. (2019) Stripy: A Python module for (constrained) triangulation in Cartesian coordinates and on a sphere. *Journal of Open Source Software*, 4(38), 1410.
- Müller, R.D., Cannon, J., Qin, X., Watson, R.J., Gurnis, M., Williams, S. et al. (2018) GPlates: building a virtual earth through deep time. *Geochemistry, Geophysics, Geosystems*, 19(7), 2243–2261. Available at: <https://doi.org/10.1029/2018GC007584>

- Muller, R.D. & Dutkiewicz, A. (2018) Oceanic crustal carbon cycle drives 26-million-year atmospheric carbon dioxide periodicities. *Science Advances*, 4(2), eaaq0500.
- Müller, R.D., Seton, M., Zahirovic, S., Williams, S.E., Matthews, K.J., Wright, N.M. et al. (2016) Ocean basin evolution and global-scale plate reorganization events since Pangea breakup. *Annual Review of Earth and Planetary Sciences*, 44(1), 107–138.
- Müller, R.D., Zahirovic, S., Williams, S.E., Cannon, J., Seton, M., Bower, D.J. et al. (2019). A global plate model including lithospheric deformation along major rifts and orogens since the Triassic. *Tectonics*, 38(6), 1884–1907. Available at: <https://doi.org/10.1029/2018TC005462>
- Pall, J., Zahirovic, S., Doss, S., Hassan, R., Matthews, K.J., Cannon, J. et al. (2018) The influence of carbonate platform interactions with subduction zone volcanism on palaeo-atmospheric CO₂ since the Devonian. *Climate of the past*, 14(6), 857–870.
- Plank, T. & Manning, C.E. (2019) Subducting carbon. *Nature*, 574(7778), 343–352.
- Ratschbacher, B.C., Paterson, S.R. & Fischer, T.P. (2019) Spatial and depth-dependent variations in magma volume addition and addition rates to continental arcs: Application to global CO₂ fluxes since 750 Ma. *Geochemistry, Geophysics, Geosystems*, 20(6), 2997–3018.
- Sleep, N.H. & Zahnle, K. (2001) Carbon dioxide cycling and implications for climate on ancient Earth. *Journal of Geophysical Research: Planets*, 106(E1), 1373–1399.
- Straume, E.O., Gaina, C., Medvedev, S., Hochmuth, K., Gohl, K., Whittaker, J.M. et al. (2019) GlobSed: updated total sediment thickness in the world's oceans. *Geochemistry, Geophysics, Geosystems*, 20(4), 1756–1772.
- Tetley, M.G., Williams, S.E., Gurnis, M., Flament, N. & Müller, R.D. (2019) Constraining absolute plate motions since the Triassic. *Journal of Geophysical Research: Solid Earth*, 124(7), 7231–7258.
- Torsvik, T.H., Steinberger, B., Shephard, G.E., Doubrovine, P.V., Gaina, C., Domeier, M. et al. (2019) Pacific-Panthalassic reconstructions: overview, errata and the way forward. *Geochemistry, Geophysics, Geosystems*, 20(7), 3659–3689.
- UNEP-WCMC, WC, WRI, TNC (2018). *Global distribution of warm-water coral reefs, compiled from multiple sources including the Millennium Coral Reef Mapping Project. Version, 4.*
- Venzke, E. (2013). *Volcanoes of the World from the Global Volcanism Program.*
- Wessel, P., Luis, J., Uieda, L., Scharroo, R., Wobbe, F. & Smith, W. et al. (2019). The generic mapping tools version 6. *Geochemistry, Geophysics, Geosystems*, 20(11), 5556–5564. <https://doi.org/10.1029/2019GC008515>
- Williams, S., Flament, N., Müller, R.D. & Butterworth, N. (2015) Absolute plate motions since 130 Ma constrained by subduction zone kinematics. *Earth and Planetary Science Letters*, 418, 66–77.
- Wong, K., Mason, E., Brune, S., East, M., Edmonds, M. & Zahirovic, S. (2019) Deep carbon cycling over the past 200 million years: a review of fluxes in different tectonic settings. *Frontiers in Earth Science*, 7, 1–22.
- Wu, L., Murphy, J.B., Quesada, C., Li, Z.-X., Waldron, J.W., Williams, S. et al. (2021) The amalgamation of Pangea: Paleomagnetic and geological observations revisited. *Bulletin*, 133(3–4), 625–646.
- Young, A., Flament, N., Maloney, K., Williams, S., Matthews, K., Zahirovic, S. et al. (2018) Global kinematics of tectonic plates and subduction zones since the late Paleozoic Era. *Geoscience Frontiers*, 10(3), 989–1013. Available at: <https://doi.org/10.1016/j.gsf.2018.05.011>
- Zahirovic, S., Matthews, K.J., Flament, N., Müller, R.D., Hill, K.C., Seton, M. et al. (2016) Tectonic evolution and deep mantle structure of the eastern Tethys since the latest Jurassic. *Earth-Science Reviews*, 162, 293–337.
- Zahirovic, S., Müller, R., Seton, M. & Flament, N. (2015) Tectonic speed limits from plate kinematic reconstructions. *Earth and Planetary Science Letters*, 418, 40–52.

SUPPORTING INFORMATION

Additional supporting information may be found in the online version of the article at the publisher's website.

How to cite this article: Zahirovic, S., Eleish, A., Doss, S., Pall, J., Cannon, J., Pistone, M., et al (2022) Subduction and carbonate platform interactions. *Geoscience Data Journal*, 00, 1–13. Available from: <https://doi.org/10.1002/gdj3.146>